ELSEVIER

Journal of Chromatography A, 969 (2002) 261–272

JOURNAL OF CHROMATOGRAPHY A

www.elsevier.com/locate/chroma

Characterisation of cement pastes by inverse gas chromatography

Victor Oliva[a], Béchir Mrabet[a,1], Maria Inês Baeta Neves[a], Mohamed M. Chehimi[a,*], Karim Benzarti[b]

[a]*Interfaces, Traitement, Organisation et Dynamique des Systèmes (ITODYS), Université Paris 7–Denis Diderot, associé au CNRS, 1 rue Guy de la Brosse, 75005 Paris, France*

[b]*Laboratoire Central des Ponts et Chaussées (LCPC), 58 boulevard Lefèbvre, 75015 Paris, France*

Abstract

Two cement pastes, commonly used in concrete formulations, were characterised by IGC at 35–80 °C before and after coating with an epoxy resin and a hardener. The cements are mixtures of hydrates in various proportions, such as calcium silicate hydrate ($CaO–SiO_2–H_2O$) and calcium hydroxide $Ca(OH)_2$. Apolar and polar probes were used to determine the dispersive and acid–base characteristics of the cement pastes. These materials have high surface energy as judged from the dispersive contribution to the surface free energy (γ_S^d) values lying in the 50–70 mJ/m^2 range at 60–80 °C. Examination of the specific interactions permitted to show that the cement pastes are strongly amphoteric species with a substantial predominant Lewis basicity that is in line with the basic pH of their aqueous suspensions. Following coating with an epoxy resin (DGEBA) and a hardener (triethylene tetramine), the surface energy of the cements decreases substantially with the mass loading of the organic material. The surface thermodynamic properties were also correlated with the surface chemical composition as determined by X-ray photoelectron spectroscopy.

Keywords: Cement paste; Inverse gas chromatography (IGC); Epoxy resin; X-ray photoelectron spectroscopy; Triethylene tetramine hardener

1. Introduction

In the field of civil engineering, polymer adhesives such as epoxy resins are getting more and more popular. At the present time, they are mainly applied to the repair of concrete structures (bridges, walls) by crack injection, or by gluing of composite or steel plates in order to restore the stiffness of the damaged structure [1,2]. Those adhesives also open up new possibilities for the design of bridges, since massive elements of the concrete structure could be assembled in the future by gluing. However, prediction of the long term durability of the adhesive joint is still hazardous since mechanisms of adhesion between concrete and polymer adhesives are not well understood. It is therefore necessary to acquire a fundamental knowledge about physico-chemical interactions that occur at concrete–polymer interfaces.

Ongoing collaborative studies are based on a physicochemical approach to the molecular interactions at concrete–polymer interfaces. However, to minimise the practical problems, the concrete has been replaced simply by cement pastes. The industrial preparation of cements is illustrated in Fig. 1. Basically, limestone and clay are ground and

*Corresponding author. Fax: +33-1-4427-6814.

E-mail address: chehimi@paris7.jussieu.fr (M.M. Chehimi).

[1]Present address: Faculté de Pharmacie, Département de Chimie, 5000 Monastir, Tunisia.

0021-9673/02/$ – see front matter
PII: S0021-9673(02)00895-6

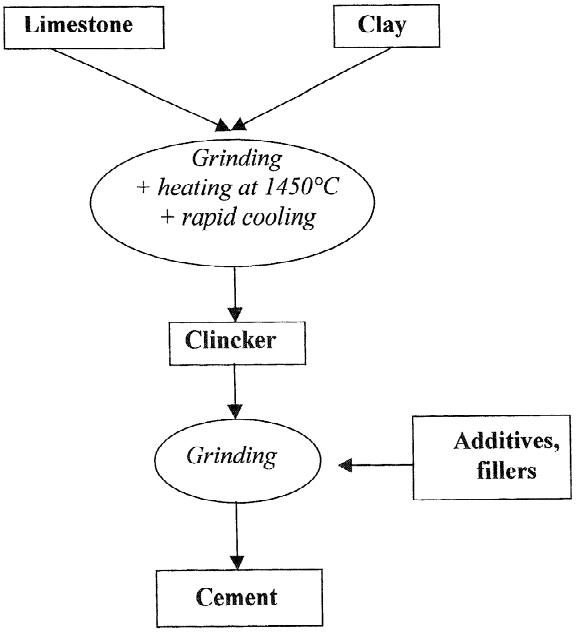

Fig. 1. Industrial preparation of cements.

heated at 1450 °C and then quickly cooled to yield a material called ''clinker''. Additives and fillers can be joined to the clinker to obtain modified cements. Cement pastes are obtained simply by mixing cement and water and then dried to solid cement pastes. The latter exhibit multi-scale porous structures (see Fig. 2), as well as complex acid–basic behaviour. These two parameters may both affect physico-chemical interactions with polymer adhesives but, to our knowledge, their influences have never been studied in the literature.

Inverse gas chromatography (IGC) is an interesting and well established technique to perform such an investigation. This tool has proved effective in characterising the surface energy of various materials such as conventional [3–5] and conducting polymers [6,7], fibres [8–10], mineral fillers [3,11] and pigments [12,13] over a wide range of temperature. It also permits to estimate the reversible work of adhesion at fiber–resin [8,14] and pigment–resin [12] interfaces. In previous studies at ITODYS, the surface energy changes of mineral and organic powders were related to the adsorption of organic polymers and silane coupling agents [15–17].

The aim of this paper is to use IGC at infinite dilution to determine γ_S^d values and acid–base descriptors of two cement pastes before and following coating with an epoxy resin of the diglycidyl ether of bisphenol A type (DGEBA) and triethylene

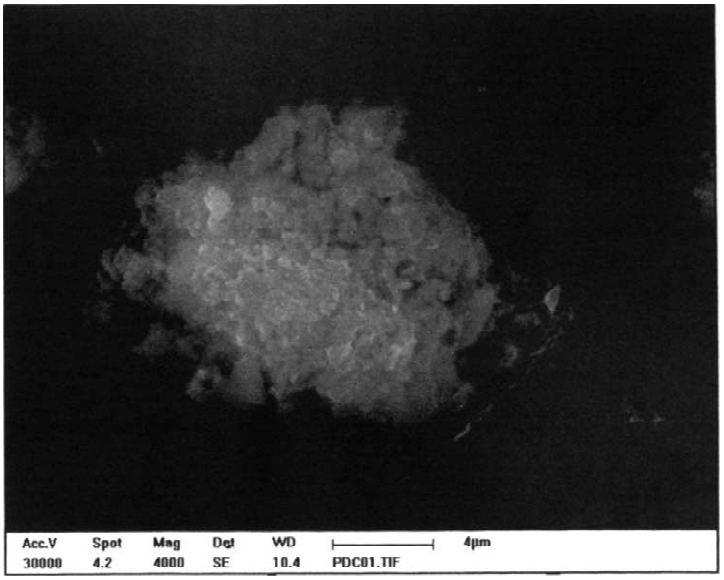

Fig. 2. SEM micrograph showing a porous and flake-like structure of a cement paste (micrograph obtained with Philips XL30 equipped with EDAX DX4, Philips Optique Electronique, Limeil-Brévannes Cedex, France).

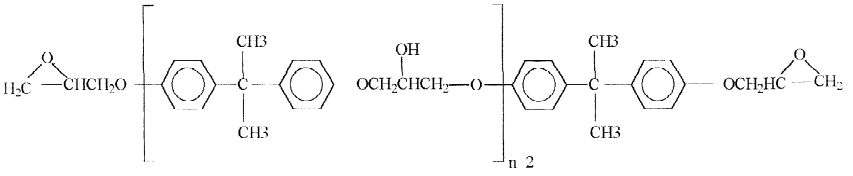

Dyglicidylether of bisphenol A (DGEBA)

$H_2N\text{-}(CH_2)_2\text{-}NH\text{-}(CH_2)_2\text{-}NH\text{-}(CH_2)_2\text{-}NH_2$

Triethylene tetramine

Fig. 3. Chemical structure of the epoxy resin and the hardener.

tetramine, used as a hardener (Fig. 3). The organic materials were coated onto Chromosorb to serve as reference materials. In addition to IGC, X-ray photoelectron spectroscopy (XPS) provided a survey of the change in the chemical composition of the cement pastes induced by the various organic coatings.

2. Experimental

2.1. Materials

Two different cements were studied, an ordinary Portland cement, CPA (industrial product CPA CEM I 52.5 PMES from Lafarge, Le Havre, France) which is almost a pure clinker and a blended cement CPJ (industrial product CPJ CEM II B 32.5 R, from Lafarge, Frangey, France) made of 71% clinker and 23% of chalky filler. These cement pastes have been prepared with a proportion of water–cement equal to 0.5 (w/w).

The resin used was of the epoxy type, namely diglycidyl ether of bisphenol A type, DGEBA (Araldite resin CY230, Ciba performance polymers, 92506 Rueil Malmaison, France) and triethylene tetramine (HY956, Ciba performance polymers, Rueil Malmaison, France) was the hardener.

For the purpose of coating the materials the well known method of Al–Saïgh and Munk [18] was chosen. The exact mass of resin (or hardener) is dissolved in 50 ml of acetone (Prolabo, Fontenay Sous Bois, France). Then, the material to be coated is placed on a clock glass or a Pétri dish and is slowly impregnated with drops of the solution acetone–resin (or hardener). The liquid must not touch the glassy vessel walls, otherwise there would be a great loss of resin (or hardener). When the solvent has evaporated the material is mixed and the whole process is repeated. This method is time consuming but is very accurate (associated error typically 1% or less) and does not require further checking by thermal gravimetric analysis or ashing [19].

2.2. Inverse gas chromatography

Stainless steel columns 30–100 cm and 1/8 in. (1 in. = 2.54 cm) outer diameter (Varian, Les Ulis, France) were packed by the fill-and-tap method with cement paste particles, Epoxy-coated cement pastes, hardener-coated cement pastes, Chromosorb-supported epoxy (5%, w/w) and Chromosorb-supported hardener (5%, w/w). The cement pastes were pellet-pressed, ground and then sieved (250–400 μm) before packing, and Chromosorb 80–100 Mesh (Celite, Lompoc, CA, USA) was used as received. A Hewlett-Packard HP6890 gas chromatograph (Waldbronn, Germany) fitted with a flame ionisation

detector was used for GC measurements. Methane (Fluka, Buchs, Switzerland) was the non-interacting marker and a high purity helium (Air Liquide, Paris La Défense, France) was the carrier gas. The flow-rate was set at 20 cm^3/min. However, a flow-rate as high as 40 ml/min was used in the case of uncoated cement pastes in order to get elution peaks of strongly adsorbed specific probes. The injector and detector temperatures were 50 and 150 °C, respectively. To avoid hardening of the cement pastes inside the columns near the outlet, it was necessary to add a very short column packed with polymethyl methacrylate (beads) which has a low specific surface area. It was found that this additional short column only shifted the dead volume but not the relative retention times. More importantly, the packing materials were found to be stable in these conditions within the time-scale of the entire analysis.

The probes were high-purity-grade *n*-alkanes, 1-alkenes, benzene and other specific acidic and basic probes. The properties of the probes are reported in Table 1 where DN [20] and AN* [21] are the Gutmann's donor and acceptor numbers.

The columns were activated at the oven temperature overnight. Air-probe vapour mixtures (1–5 μl) were injected manually by a gas-tight syringe. Fig. 4 depicts elution peaks for *n*-alkanes, benzene and tetrahydrofuran (THF) injected together with the reference probe methane (C_1) in a column loaded with CPA particles. The retention times were determined at the peak maximum for symmetrical peaks. For skewed or tailing peaks, retention times were determined at the mass centre of the peak. Extrapolation to zero coverage was necessary in the case of concentration-dependent retention.

2.3. X-ray photoelectron spectroscopy

A VG Escalab MK1 spectrometer (East Grinstead, UK) equipped with a twin anode was used. Polychromatic Al Kα X-ray source (1486.6 eV) has been selected and operated at a power of 200 W (10 kV with an emission current of 20 mA). The pass energy was set at 50 eV. The pressure in the analysis chamber was $\approx 10^{-8}$ mbar. The data were collected with Pisces software (Dayta Systems, Bristol, UK). The step size was 1 and 0.1 eV for the survey and the narrow scans, respectively.

Data processing was achieved with a Winspec software, kindly supplied by the Laboratoire Interdisciplinaire de Spectroscopie Electronique (LISE,

Table 1
Probes used to characterise the various materials

Probes	Abbreviation	bp (°C)	DN[a]	AN*[a]	Supplier[b]
n-Pentane	C_5	36.1	–	–	Prolabo
n-Hexane	C_6	68.7	–	–	Prolabo
n-Heptane	C_7	98.4	–	–	Prolabo
n-Octane	C_8	125.7	–	–	Fluka
n-Nonane	C_9	150.8	–	–	Fluka
n-Decane	C_{10}	174.1	–	–	Fluka
Trimethyl butane	TMB	80.9	–	–	Aldrich
1-Pentene	Π_5	30.0	–	–	Aldrich
1-Hexene	Π_6	63.3	–	–	Aldrich
1-Heptene	Π_7	94.0	–	–	Aldrich
Chloroform	$CHCl_3$	61.2	0	22.6	Aldrich
Carbon tetrachloride	CCl_4	77.0	0	2.3	Prolabo
Diethylether	DEE	34.6	80.3	5.9	Prolabo
Acetonitrile	AN	81.0	59.0	19.7	Prolabo
Benzene	Bnz	80.0			Prolabo
Methyl acetate	MeAc	57.4	69.0	6.9	Janssen
Methanol	MeOH	65.0		50.2	Prolabo
Tetrahydrofuran	THF	66.0	83.7	2.1	Prolabo

[a] DN and AN* are in kJ/mol.
[b] Prolabo (Fontenay Sous Bois, France), Fluka (Buchs, Switzerland), Aldrich (Steinheim, Germany), Janssen (Geel, Belgium).

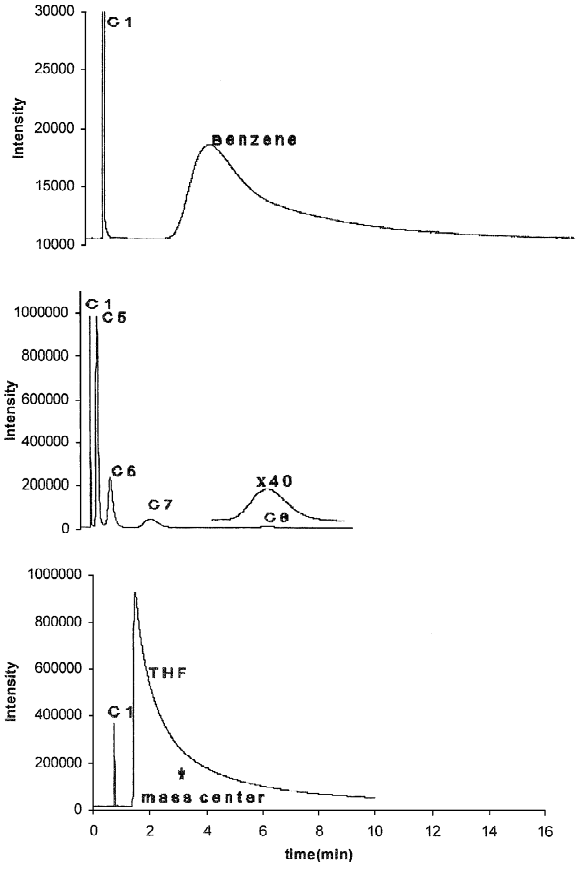

Fig. 4. Elution peaks for *n*-alkanes, benzene and THF.

Namur, Belgium). The spectra were corrected for static charging by setting the C1s peak maximum at 285 eV. The surface composition was determined using experimental sensitivity factors. The fractional concentration of a particular element A (% A) was computed using:

$$\%\,A = \frac{(I_A/s_A)}{\sum(I_n/s_n)} \cdot 100$$

where I_n and s_n are the integrated peak areas and the sensitivity factors, respectively.

3. Results and discussion

3.1. X-ray photoelectron spectroscopy

Fig. 5 shows the XPS survey spectra of a CPJ

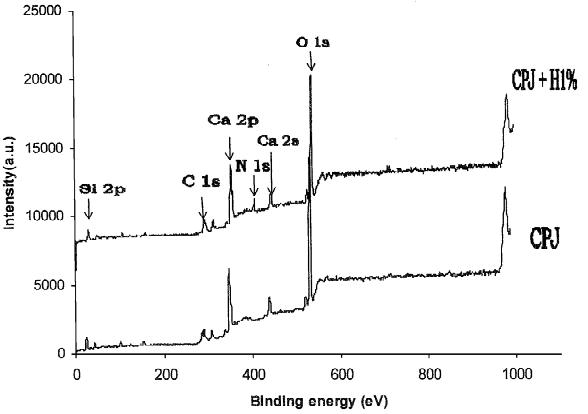

Fig. 5. XPS survey spectra of a CPJ cement paste before and following coating with the hardener at a mass loading of 1% (H1%).

cement paste before and following coating with the hardener. The most important peaks are Si2p, Ca2p, O1s and C1s centred at 103, 347, 531 and 285 eV, respectively. The hardener exhibits a N1s peak centred at 400 eV. The surface composition was practically the same after pressing and grinding the cement paste and also after IGC characterisation.

Table 2 shows the surface composition (in atom%) of the various materials as determined by XPS. The carbon content (% C) invariably increases at the surface of CPA and CPJ following organic coating with either epoxy or hardener. In the case of coating with 5% (w/w) epoxy, % C is twice as high as for uncoated CPA and 50% higher than for uncoated CPJ. There is also a slight decrease of the oxygen content after coating due to the attenuation of the calcium silicates and other oxides. The decrease in the calcium content is very small but measurable,

Table 2
Surface composition as determined by XPS (in atom%) of the cement pastes before and after coating

Materials	Ca	Si	O	C	N
CPA	19.6	6.32	60.5	13.6	–
CPA–H1%	15.7	4.03	50.0	25.1	5.14
CPA–R1%	16.1	1.98	52.1	29.8	–
CPA–R5%	16.8	4.50	52.8	25.9	–
CPJ	17.2	3.73	59.8	19.3	–
CPJ–H1%	16.3	3.60	54.7	22.2	3.17
CPJ–R1%	17.9	2.87	55.8	23.4	–
CPJ–R5%	15.7	4.02	52.7	27.6	–

whereas the silicon content has not a clear variation with organic coating especially in the case of CPJ.

3.2. Inverse gas chromatography

The surface energy of the cement pastes was studied using *n*-alkanes, trimethylbutane, 1-alkenes, CCl_4, and a range of Lewis acids and bases. Fig. 6 depicts plots of $RT \ln V_N$ values vs. the number of carbon atoms in the *n*-alkane series for CPA and CPJ pastes at 35 and 80 °C. The slopes which measure $\Delta G_a^{CH_2}$, the free energy of adsorption per methylene group, are quasi-identical for the two cements and temperature-independent despite the 45 °C difference between the two working temperatures.

Using the approach of Dorris and Gray [22] we computed γ_s^d values:

$$\gamma_S^d = (1/4\gamma_{CH_2})\left(\Delta G_a^{CH_2}/Na_{CH_2}\right)^2 \quad (1)$$

where N is the Avogadro number and a_{CH_2} is the cross-sectional area of an adsorbed CH_2 group (6 $Å^2$). γ_{CH_2} is the surface free energy of a solid containing only methylene groups such as polyethylene, and is expressed by [22]:

$$\gamma_{CH_2} = 36.8 - 0.058T \ (°C) \quad (2)$$

Fig. 7 shows the trends of γ_S^d values for CPA paste. The values are in the 54–67 mJ/m^2 range at 35–80 °C, using a flow-rate of 40 ml/min. Setting the flow-rate at a lower value (25 ml/min), we found a higher γ_S^d of 81.8 mJ/m^2 at 60 °C (after 15 h of conditioning). There is a clear evidence for the effect of flow-rate. Probably 40 ml/min is a too high flow-rate which prevents the adsorption–desorption equilibria of the *n*-alkanes to be established properly. This is exacerbated for a thorough conditioning at 150 °C for 4 h as γ_S^d reached a value of 90.6 mJ/m^2, typical characteristic of fairly high surface energy material such as oxides and clays, namely silica (98.2 mJ/m^2 at 20 °C) [23], MgO (95.6 mJ/m^2 at 25 °C) [24], and γ-alumina (92 mJ/m^2 at 100 °C) [25] and smectite (159 mJ/m^2 at 180 °C) [26].

The working and also the conditioning temperature has an important effect. Indeed, the γ_S^d value increases with the working temperature an indication that the surface gets activated by desorbing adventitious hydrocarbon contamination and probably adsorbed water. This result is contrary to the expected behaviour of materials surfaces which normally exhibit a decrease of the γ_S^d values with temperature. Nevertheless, Keller and Luner [27] determined for calcium carbonate a γ_S^d value of 55 mJ/m^2 at 100 °C after a conditioning at 50 °C, and a value as high as

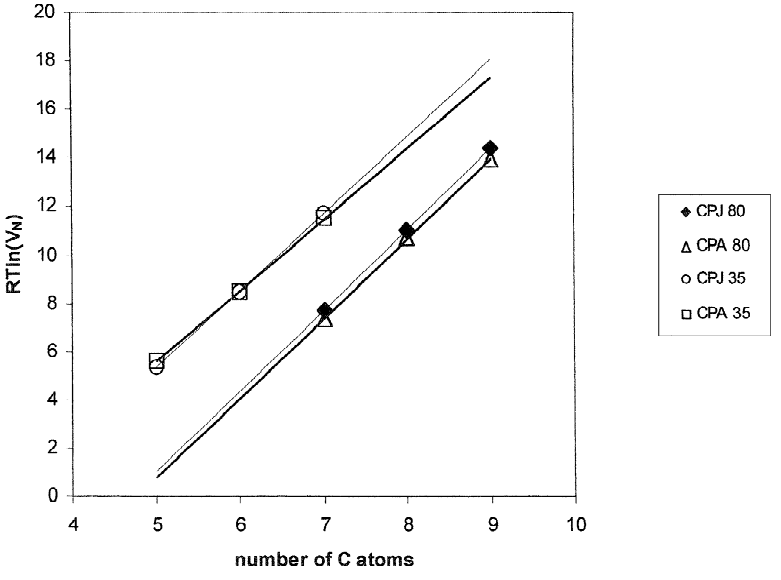

Fig. 6. Plots of $RT \ln V_N$ values vs. the number of carbon atoms in the *n*-alkane series for CPA and CPJ pastes at 35 and 80 °C.

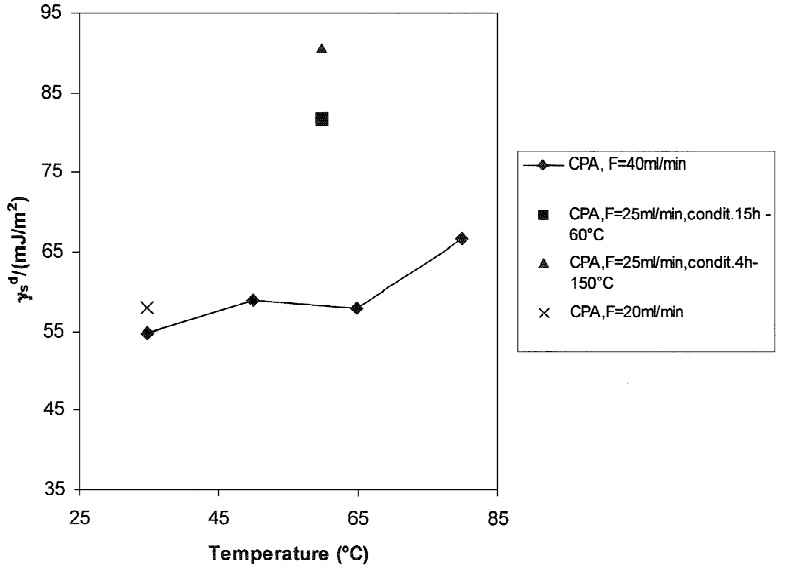

Fig. 7. Trends of γ_S^d values for CPA paste. Effect of flow-rate and conditioning temperature.

255 mJ/m^2 after a conditioning at 200 °C. They assigned this behaviour to water desorption from the most energetic surface sites.

Acid–base interactions were studied using the traditional approach of Brookman and Sawyer [28] in which ΔG_a or $RT \ln V_N$ values of the various injected probes are related to the boiling temperature (bp). This is illustrated in Fig. 8 where the *n*-alkanes series lead to a reference linear correlation that accounts for dispersive interactions. For specific probes the corresponding $RT \ln V_N$ values deviate from the dispersion force reference line by a vertical

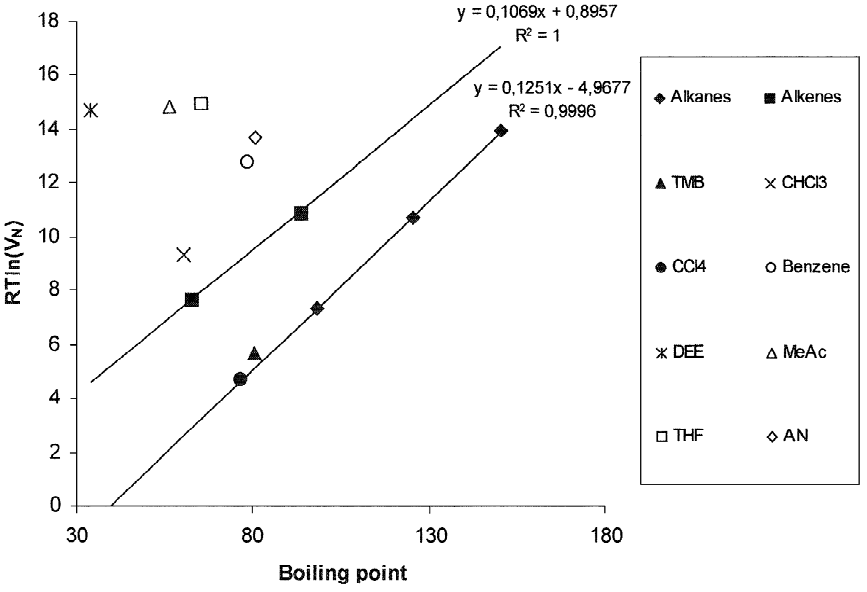

Fig. 8. Plot of $RT \ln V_N$ values vs. boiling temperature (bp) for the various injected probes.

distance that accounts for the acid–base contribution to the free energy of adsorption:

$$-\Delta G_a^{AB} = RT \ln V_N/V_{N,ref} \quad (3)$$

where $V_{N,ref}$ is the net retention volume of an hypothetical *n*-alkane which boils at the same temperature as the test polar probe. $-\Delta G_a^{AB}$ is also defined as I_{sp}, the specifc interaction parameter.

For CPA at 80 °C (Fig. 8), an excellent linear plot is generated with *n*-alkanes. TMB is a branched alkane and has its corresponding $RT \ln V_N$ value 0.51 kJ/mol unit above the dispersion interaction plot, thus matching that of a hypothetical *n*-alkane that boils at 80.9 °C. This indicates that there is no effect of microporosity on the retention of probes. Actually, when micropores are accessible to *n*-alkanes and not branched alkanes, the latter have retention data below the reference *n*-alkane line [7] because they interact only with the materials surface and are excluded from the adsorption sites located in the micropores.

1-Alkenes yield a linear plot that is above the one of the *n*-alkanes. This means that the 1-alkenes interact specifically with the sorbent. However, the lower slope is the result of a decrease of the π electronic density with increasing chain length. CCl_4 marker is close to the *n*-alkane line indicating that this probe interacts with cement pastes via weak specific acid–base bonds. In contrast, for all other specific probes, the markers are lying much above the *n*-alkane reference line, a qualitative indication of strong acid–base probe-adsorbent interactions.

Table 3 reports I_{sp} values for specific probes at 80 °C.

One can classify the specific probes in a increasing series of specific interaction energies (I_{sp}):

$$CCl_4 < \text{alkenes} < \text{benzene} < CHCl_3 < \text{AN} < \text{THF} < \text{MeAc} < \text{DEE}$$

Acidity (K_A) and basicity (K_B) were calculated using a semi-quantitative method:

$$I_{sp} = K_A \cdot \text{DN} + K_B \cdot \text{AN}^* \quad (4)$$

where DN and AN* are the donor and acceptor numbers of the reference solutes. Eq. (4) is based on the approach of Saint Flour and Papirer [29] but relates ΔG_a^{AB}, and not ΔH_a^{AB} (the heat of acid–base adduct formation) to Gutmann's numbers.

Eq. (4) can be rearranged in the following manner:

$$I_{sp}/\text{AN}^* = K_A \cdot \text{DN}/\text{AN}^* + K_B \quad (5)$$

where the unknowns K_A and K_B can be calculated graphically.

Fig. 9 shows a linear plot of I_{sp}/AN* versus DN/AN* of which slope and intercept equal to K_A and K_B, respectively. $K_A \times 100 = 12.4$ and $K_B \times 100 = 40.9$, with $K_B/K_A = 3.3$. This ratio accounts for a predominant basicity of the surface. Indeed, for PVC (acidic polymer) and PMMA (basic) the ratio is 1.46 and 4.7, respectively [17]. This is in line with the basic pH of 12 units found for CPA aqueous suspensions.

We shall consider now organic coatings of epoxy resin (1 and 5%, w/w; R1% and R5%) and a hardener (1%, w/w; H1%) from acetone onto CPA and CPJ. Since organic coatings are low energy materials, the results presented below were all obtained using a flow-rate of 20 ml/min and a working temperature of 35 °C, comparable to the temperature that is used in practice with these inorganic and organic materials. It should be noted at this stage that only *n*-alkane adsorption characteristics will be presented as our aim was only to see in which manner the organic materials coat the cement pastes, in other words, to see whether they coat the substrates with continuous or patchy overlayers. Obviously, this can be easily detected by the determination of γ_S^d values. A decrease in these values is

Table 3
Specific interaction energy (I_{sp}) values of the specific probes injected on CPA and CPJ cement pastes at 80 °C

Cement	Probes								
	CCl_4	Π_6	Π_7	$CHCl_3$	Bnz	THF	AN	DEE	MeAc
CPA	0.08	4.71	4.06	7.87	7.84	10.9	7.78	14.8	7.78
CPJ	0.500	4.44	3.52	7.13	–	–	–	–	–

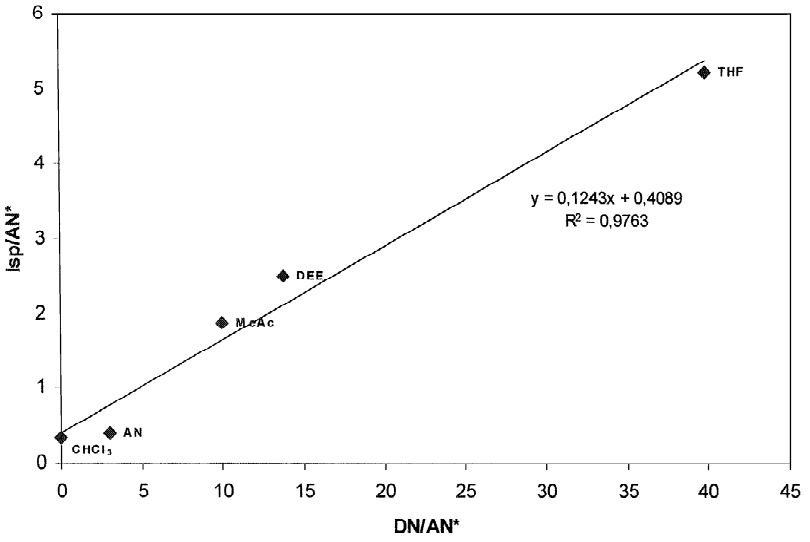

Fig. 9. Linear plot of I_{sp}/AN* versus DN/AN*. Determination of K_A and K_B for CPA at 80 °C.

expected as we start with a fairly high energy material that is coated with low energy materials. In real situations, both Epoxy resin and hardener are mixed to glue concrete parts. However, during cure, preferential adsorption at interfaces may occur and it is thus important to compare adsorption and wetting of the cement pastes by the epoxy and the hardener separately.

Fig. 10 shows plots of $RT \ln V_N$ values vs. the number of carbon atoms in the *n*-alkanes for CPA, CPA–R1%, CPA–R5%, CPA–H1% and R5% (coated on Chromosorb). There is a significant

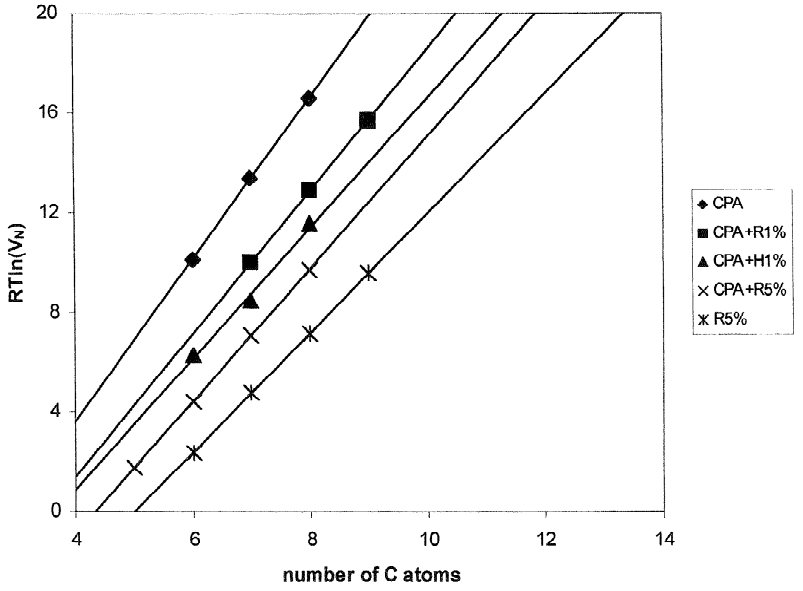

Fig. 10. Plots of $RT \ln V_N$ values vs. the number of carbon atoms for uncoated and coated CPA cement pastes and the reference epoxy resin at 35 °C (flow-rate: 20 ml/min).

change in the slopes on going from the uncoated CPA cement to the coated ones. Increasing the load in the resin yields an even much lower slope.

Fig. 11 depicts a plot of γ_S^d values for CPA and CPJ before and after coating with the resin and the hardener. For 5% (w/w) loading, the decrease in γ_S^d is slightly more important for CPA. It is worth to note that 1% (w/w) hardener decreases the energy of CPA in a similar manner than 5% (w/w) resin, perhaps suggesting a better wetting of the cements by the hardener than by the resin.

However, in the case of CPJ, the coating with the hardener did not lead to a significant decrease of γ_S^d values and this is perhaps due to a different wetting quality. Indeed, the surface chemical composition indicates less nitrogen and carbon concentration, for the same mass loading of hardener, than on CPA.

In order to relate the surface energy to the surface chemistry of the materials, γ_S^d values (at 35 °C) were plotted versus the (C+N)/(Ca+Si+O) atomic ratio as determined by XPS (Fig. 12). This atomic ratio was chosen as a semi-quantitative measure of organic-to-inorganic material content. One can note a distinct decreasing trend of the surface energy with the concentration of elements characteristic of organic materials loaded on the cement pastes.

4. Conclusion

IGC has been applied for the first time to characterise cement pastes, materials used in the civil engineering field. Cement pastes behave as high energy materials and are amphoteric with a predominant basicity. Coating with epoxy resin and a hardener resulted in a decrease of the surface energy as a function of the mass loading of the organic materials. The two cements behave in a similar manner either bare or coated with the Epoxy resin. Interestingly, it was found that the hardener decreases more significantly the surface energy of CPA cement than the resin, perhaps indicating a better wetting.

These findings are of technological importance since these cements are intended for concrete assemblies using high-performance adhesives.

5. Nomenclature

IGC	inverse gas chromatography
XPS	X-ray photoelectron spectroscopy
CPA	ordinary Portland cement
CPJ	blended cement

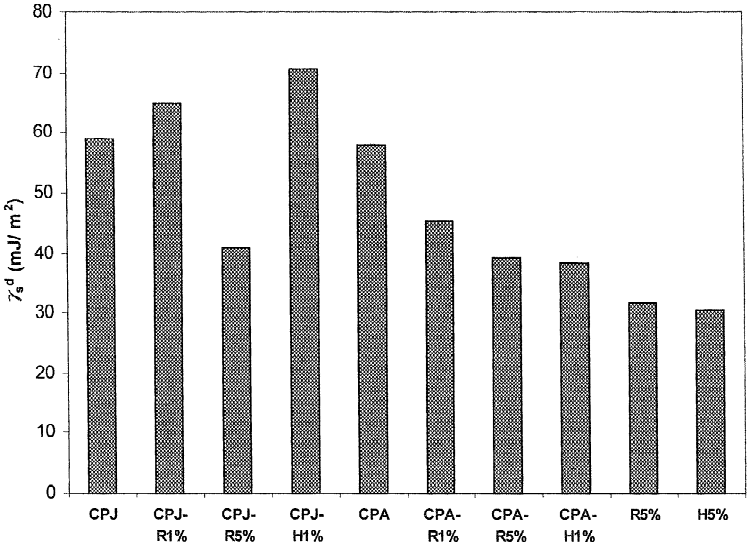

Fig. 11. Variation of γ_S^d values for CPA and CPJ with organic coatings (resin and hardener).

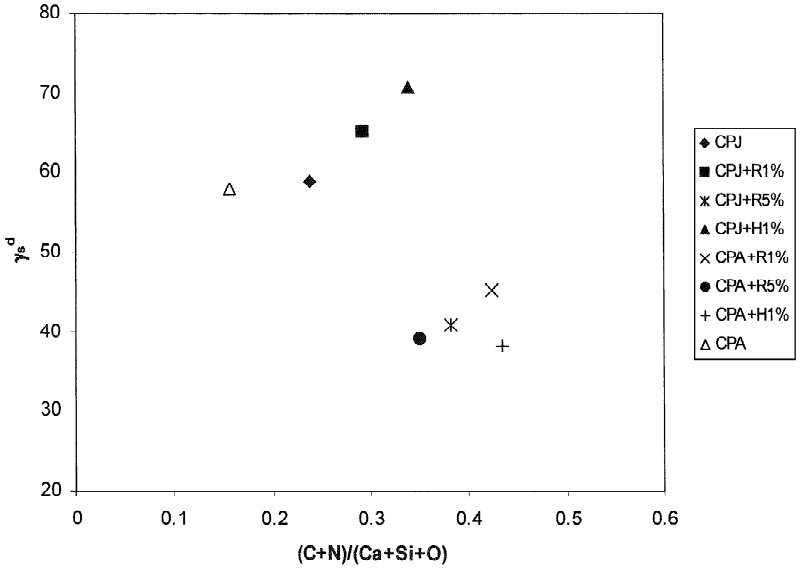

Fig. 12. Relationship between IGC and XPS: plot of γ_S^d values (at 35 °C) versus the (C+N)/(Ca+Si+O) atomic ratio for uncoated and coated CPA and CPJ cement pastes.

R1%	1% (w/w) of epoxy resin
R5%	5% (w/w) of epoxy resin
H1%	1% (w/w) of hardener
H5%	5% (w/w) of hardener
DGEBA	epoxy resin of the diglycidyl ether of bisphenol A type
γ_S^d	dispersive contribution to the surface free energy
γ_{CH_2}	surface free energy of a methylene group
$\Delta G_a^{CH_2}$	free energy of adsorption per methylene group
N	Avogadro number
a_{CH_2}	cross-sectional area of an adsorbed CH_2 group (6 $Å^2$)
T	temperature
R	gas constant
V_N	net retention volume
$V_{N,ref}$	net retention volume of an hypothetical *n*-alkane that boils at the same temperature than the test polar probe
bp	boiling temperature
ΔG_a^{AB}	acid–base contribution to the free energy of adsorption
ΔH_a^{AB}	heat of acid–base adduct formation
I_{sp}	specific interaction parameter
K_A	Lewis acidity
K_B	Lewis basicity
DN	Gutmann's donor number
AN*	Gutmann's acceptor number, corrected for Van der Waal's interactions

Acknowledgements

The authors would like to thank LCPC and Université Paris 7 for financial support (research project no. 2000-C0061) and Carole Connan for technical assistance with XPS measurements.

References

[1] V.M. Karhari, L. Zhao, Comput. Methods Appl. Mech. Eng. 185 (2000) 433.
[2] J.-N. Theillout, in: Proceedings of the Symposium RILEM ISAP 86, Chapman & Hall, London, 1986, p. 601.
[3] M.N. Belgacem, A. Gandini, Surfact. Sci. Ser. 80 (1999) 41.
[4] Z. Al-Saigh, Polym. News 19 (1994) 269.
[5] C. Demathieu, M.M. Chehimi, J.-F. Lipskier, Sensors Actuators B 62 (2000) 1.

[6] M.M. Chehimi, M.-L. Abel, C. Perruchot, M. Delamar, S.F. Lascelles, S.P. Armes, Synth. Metals 104 (1999) 51.
[7] C. Perruchot, M.M. Chehimi, M. Delamar, S.F. Lascelles, S.P. Armes, J. Colloid Interface Sci. 193 (1997) 190.
[8] B. Riedl, H. Chtourou, Surfact. Sci. Ser. 80 (1999) 125.
[9] P.E. Vickers, J.F. Watts, C. Perruchot, M.M. Chehimi, Carbon 38 (2000) 675.
[10] R.E. Allred, S.P. Wesson, in: K.L. Mittal (Ed.), Acid–base Interactions: Relevance To Adhesion Science and Technology, Vol. 2, VSP, Utrecht, 2000, p. 551.
[11] E. Papirer, H. Balard, Surfact. Sci. Ser. 80 (1999) 145.
[12] J. Lara, H.P. Schreiber, J. Coat. Technol. 63 (1991) 81.
[13] V. Lavaste, J.F. Watts, M.M. Chehimi, C. Lowe, Int. J. Adhesion Adhesives 20 (2000) 1.
[14] J. Schultz, L. Lavielle, C. Martin, J. Adhesion 23 (1987) 45.
[15] M.M. Chehimi, M.-L. Abel, Z. Sahraoui, J. Adhesion Sci. Technol. 10 (1996) 287.
[16] M.M. Chehimi, M.-L. Abel, J.F. Watts, R.P. Digby, J. Mater. Chem. 11 (2001) 533.
[17] M.-L. Abel, M.M. Chehimi, F. Fricker, M. Delamar, A.M. Brown, J.F. Watts, J. Chromatography A (2002) in press.
[18] Z. Al-Saigh, P. Munk, Macromolecules 17 (1984) 803.
[19] C. Demathieu, PhD thesis, Université Paris 7, 1998.
[20] V. Gutmann (Ed.), The Donor–Acceptor Approach to Molecular Interactions, Plenum Press, New York, 1978.
[21] F.L. Riddle Jr., F.M. Fowkes, J. Am. Chem. Soc. 112 (1990) 3259.
[22] G.M. Dorris, D.G. Gray, J. Colloid Interface Sci. 77 (1980) 353.
[23] A. Vidal, E. Papirer, M.J. Wang, J.B. Donnet, Chromatographia 23 (1987) 121.
[24] J. Kuczynski, E. Papirer, Eur. Polym. J. 27 (1991) 653.
[25] E. Papirer, G. Linger, H. Balard, A. Vidal, F. Mauss, in: D.E. Leyden, W.T. Collins (Eds.), Chemically Modified Oxide Surfaces, Gordon and Breach, New York, 1990, p. 15.
[26] T.J. Bandosz, J. Jagiello, B. Anderson, J.A. Schwarz, Clays Clay Miner. 40 (1992) 306.
[27] D.S. Keller, P. Luner, Colloids Surf. A 161 (2000) 401.
[28] D.J. Brookman, D.T. Sawyer, Anal. Chem. 40 (1968) 106.
[29] C. Saint Flour, E. Papirer, Ind. Eng. Chem. Prod. Rev. 21 (1982) 666.